Environ. Sci. Technol. **2009,** *43,* 6996–7002

Coupled Factors Influencing Concentration-Dependent Colloid Transport and Retention in Saturated Porous Media

SCOTT A. BRADFORD,*,† HYUNJUNG N. KIM,‡ BERAT Z. HAZNEDAROGLU,‡ SAEED TORKZABAN,§ AND SHARON L. WALKER‡

United States Department of Agriculture, Agricultural Research Service, United States Salinity Laboratory, Riverside, CA 92507, Department of Chemical and Environmental Engineering, University of California, Riverside, CA 92521, and Earth Sciences Division, Lawrence, Berkeley National Laboratory, Berkeley, CA 94720

Received March 19, 2009. Revised manuscript received June 22, 2009. Accepted July 23, 2009.

Downloaded by U OF CALIFORNIA RIVERSIDE on September 11, 2009 | http://pubs.acs.org
Publication Date (Web): August 11, 2009 | doi: 10.1021/es900840d

The coupled influence of input suspension concentration (C_i), ionic strength (IS), and hydrodynamics on the transport and retention of 1.1 μm carboxyl-modified latex colloids in saturated quartz sand (150 μm) under unfavorable attachment conditions (pH 10) was investigated. The percentage of retained colloids in column experiments decreased with C_i at intermediate IS conditions (31 or 56 mM) when colloids were weakly associated with the solid phase by a shallow secondary energy minima. In contrast, the effects of C_i on colloid retention were absent when IS was too low (6 mM) or too high (106 mM). The concentration effects under intermediate IS conditions were dependent on the system hydrodynamics, magnitude of C_i, and injection order of C_i, but they were largely independent of the input colloid mass. These observations were explained in part by time- and concentration-dependent filling of retention sites. Only a small fraction of the solid surface area was found to contribute to retention when IS was 31 mM, and micromodel observations indicated that colloid retention was enhanced in lower velocity regions of the pore space that occurred near grain−grain contacts. Consequently, retention profiles for IS = 31 mM conditions were increasingly nonexponential at lower values of C_i (during filling), whereas the observed concentration effect was largely eliminated as retention locations became filled. In addition, micromodel observations indicated that liquid and solid phase mass transfer of colloids to retention locations was influenced by C_i under intermediate IS conditions. Higher values of C_i are expected to produce less relative mass transfer to retention locations due to increased numbers of collisions that knock weakly associated colloids off the solid phase. Hence, the concentration effects were found to be largely independent of input colloid mass during filling of retention sites.

* Corresponding author phone: 951-369-4857; e-mail: Scott.Bradford@ars.usda.gov.
† United States Salinity Laboratory.
‡ University of California.
§ Berkeley National Laboratory.

Introduction

Aqueous concentrations of colloids vary widely in the environment as a result of differences in source as well as hydrologic, geochemical, and microbiological conditions (*1*−*4*). The potential influence of colloid concentration on the transport and fate of colloids in porous media has typically been neglected in studies that are designed to understand specific mechanisms of colloid retention. However, a limited number of studies have demonstrated that colloid concentration can have a large influence on the rates and mechanisms of colloid retention (*5*−*12*).

Results from previous studies regarding the effects of colloid concentration on retention have demonstrated a complex interplay between colloid concentration, pore size and geometry, colloid size, and aqueous phase velocity (*9, 12*). Furthermore, a variety of colloid retention mechanisms have been implicated in these studies that have time- and concentration-dependent behavior (*10, 12*). It is possible that the impact of colloid concentration is 2-fold, contributing to attachment and straining processes. Attachment involves collision with a solid−water interface and retention via adhesive forces. Time- and concentration-dependent attachment coefficients have been reported in the literature as a result of "blocking" or "ripening" (*8, 13*).

Straining processes involve colloid retention at or near multiple interfaces (*14*), and the potential for concentration effects is therefore dependent on the system geometry. When multiple colloids collide and are retained in a pore constriction, colloid retention has been reported to increase with increasing hydrodynamic forces and colloid concentration (*9, 11*) due to jamming and plugging of the pore constriction. In contrast, the colloid mass flux, pore space geometry, and system hydrodynamics are very different near grain−grain contacts (*15*). In particular, colloids that are weakly associated with the solid phase may be funneled by hydrodynamic forces toward these locations (*15*−*17*). In this case, increasing amounts of relative colloid (to the input concentration) retention have been observed with decreasing colloid concentration (*12*).

It should be mentioned that straining processes have traditionally been assumed to be purely a physical phenomena (*17, 18*) and, therefore, only determined by geometry considerations. Recent experimental evidence, however, indicates a strong coupling of straining processes on solution chemistry and hydrodynamics (*19*−*22*). The potential coupled influence of solution chemistry and colloid concentration on straining has not yet been reported in the literature. It is also possible that colloid aggregation may play a role in colloid retention at straining locations (*23, 24*), and this process is expected to be a function of hydrodynamics and the chemistry of the colloids and solution (*14*).

Although the above literature indicates that time- and concentration-dependent colloid transport and retention has previously been observed, our understanding of and ability to predict such behavior is limited because of the complex coupling of many relevant factors. The objective of this work is to investigate the coupled influence of colloid concentration with solution chemistry and hydrodynamics on retention mechanisms in packed bed column and micromodel experiments. Specific solution chemistry conditions are identified when concentration-dependent colloid transport is expected. Results from this work also have important implications for quantifying the evolution of the colloid retention profile over time, for determining the potential importance of transients

10.1021/es900840d CCC: $40.75 © 2009 American Chemical Society
Published on Web 08/11/2009

TABLE 1. Column Properties[a]

figure	IS (mM)	C_i (N_c mL^{-1})	q (cm min^{-1})	ε	L_c (cm)	T_o (PV)	M_{BTC} (%)
1a	6	3.6×10^6	0.09	0.37	13.2	1.4	93
1a	6	3.6×10^9	0.10	0.37	13.2	1.5	91
1b	31	3.6×10^6	0.12	0.41	13.6	1.6	5
1b	31	3.6×10^7	0.12	0.41	13.7	1.6	3
1b	31	3.6×10^8	0.14	0.39	13.1	2.0	67
1b	31	3.6×10^9	0.12	0.36	12.5	2.1	92
2a	31	3.6×10^6	0.56	0.36	13.0	1.8	33
2a	31	3.6×10^9	0.57	0.36	13.1	1.8	78
S3[b]	31	3.6×10^7	0.25	0.37	13.3	19.3	32
S3[b]	31	3.6×10^8	0.25	0.37	13.1	1.9	85
1c	56	3.6×10^6	0.12	0.41	13.6	1.6	6
1c	56	3.6×10^7	0.11	0.41	13.7	1.4	2
1c	56	3.6×10^8	0.11	0.39	13.1	1.7	3
1c	56	3.6×10^9	0.10	0.36	12.5	1.7	31
2b	56	3.6×10^6	0.56	0.37	13.3	1.7	7
2b	56	3.6×10^9	0.61	0.35	12.9	2.0	42
1d	106	3.6×10^6	0.10	0.37	13.2	1.5	0
1d	106	3.6×10^9	0.09	0.36	13.0	1.5	0
4	31	MP1[c]	0.52	0.36	12.9	PV1[d]	52, 81, 85, 112
S3a[b]	31	MP2[e]	0.26	0.37	13.3	1.9	38, 65
S3b[b]	31	MP3[f]	0.25	0.36	13.1	1.9	58, 39, 88, 105

[a] Properties include porosity, ϵ; column length, L_c; Darcy velocity, q; pulse duration, T_o, in terms of pore volume, PV, and percent recovery in the BTC (M_{BTC}) for each experimental system. [b] Figure is in the Supporting Information. [c] MP1 = C_i pulses of 3.6×10^7, 3.6×10^9, 3.6×10^8, and 3.6×10^7 N_c mL^{-1}. [d] PV1 = 1.7, 1.3, 3.4, and 2.5 PV. [e] MP2 = C_i pulses of 3.6×10^6, 3.6×10^8 N_c mL^{-1}. [f] MP3 = C_i pulses of 3.6×10^8, 3.6×10^7, 3.6×10^9, 3.6×10^7 N_c mL^{-1}.

in suspension concentration on colloid fate, and for predicting long-term colloid transport.

Materials and Methods

Experiments used aqueous solutions of NaCl for the eluting and resident solutions and NaBr for the tracer solution. To achieve highly unfavorable attachment conditions, we used solutions consisting of deionized (DI) water with its pH adjusted to 10 using 1.7 mM of Na_2CO_3 and 1.7 mM of $NaHCO_3$. Four ionic strength (IS) levels were considered in the experiments: 6, 31, 56, and 106 mM.

Fluorescent (excitation at 505 nm, emission at 515 nm) carboxyl-modified latex (CML) microspheres (Molecular Probes, Eugene, OR) were used in the colloid studies. The microspheres are reported by the manufacturer to be 1.1 μm in size and hydrophilic, with a density of 1.05 g cm^{-3}. The uniformity of the colloid size was verified using a Horiba LA 930 (Horiba Instruments, Inc., Irvine, CA) laser scattering particle size and distribution analyzer. The zeta potential of these microspheres in the various solution chemistries was calculated from experimentally measured electrophoretic mobilities using a ZetaPALS instrument (Brookhaven Instruments Corporation, Holtsville, NY) and the Smoluchowski equation. Colloid suspension input concentrations (C_i) used in experiments (Table 1) ranged over 3 orders of magnitude (from 3.6×10^6 to 3.6×10^9 N_c mL^{-1}, where N_c is the number of colloids). Average (three measurements) colloid concentrations reported herein were determined using a Turner Quantech fluorometer (Barnstead/Thermolyne, Dubuque, IA), and reproducibility was typically within 1% of C_i.

Ottawa sand was employed in transport and batch studies. Ottawa sand, which is a natural aquifer material reported to consist of 99.8% SiO_2 (quartz) and trace amounts of metal oxides, is spheroidal in shape with a rough surface. Quartz and iron oxides possess a net negative charge at pH 10, and any attractive electrostatic interactions between the colloids and porous medium are expected to be minimized at this pH. The median grain size of the sand was 150 μm, and the coefficient of uniformity was 2.25. The zeta potential of these sands under the various solution chemistry conditions was estimated from literature values measured for quartz sand (*25*, *26*).

The total interaction energy of the 1.1 μm CML colloids upon approach to a quartz surface under various solution chemistries (pH 10, IS = 6, 31, 56, and 106 mM) was calculated using the Derjaguin−Landau−Verwey−Overbeek (DLVO) theory and a sphere−plate assumption (*27*, *28*). Electrostatic double layer interactions were quantified using the expression of Hogg et al. (*29*) using zeta potentials in place of surface potentials. The retarded London−van der Waals attractive interaction force was determined from the expression of Gregory (*30*) utilizing a value of 4.04×10^{-21} J for the Hamaker constant (*31*).

Batch experiments were conducted by placing 10 g of sand and 10 mL of a colloid suspension with a known C_i (3.6×10^6 or 3.6×10^9 N_c mL^{-1}) and IS into a 20 mL glass scintillation vial. The suspension and sand were allowed to equilibrate for 4 h at 8 rpm using an orbital shaker (Lab-Line, Melrose Park, IL), and the final colloid concentration (C_f) was measured. All batch experiments were replicated, and blanks were run to determine the background interference from the sand. The retention of colloids in the batch system (R_B) was determined as $1 - (C_f/C_i)$.

Procedures and protocols for obtaining the breakthrough curves (BTCs) and retention profiles (RPs) in the saturated packed column (15 cm long and 4.8 cm inside diameter) experiments are reported in detail by Bradford et al. (*20*, *32*) and are in the Supporting Information. Table 1 provides values of porosity (ε), column length (L_c), Darcy velocity (q), colloid pulse duration (T_o) in terms of pore volume (PV), and the percent recovery of injected colloids in the breakthrough curve (M_{BTC}) for each experiment. Most of the transport experiments were replicated, and this information is summarized in Table S1 of the Supporting Information. Replicate experiments conducted with the same batch of colloids exhibited very good reproducibility as demonstrated in Figure S1 of the Supporting Information. Differences in the replicate column experiments were more pronounced when using a new batch of colloids, presumably due to slight variations in colloid properties. To overcome this limitation, we based the figures and data comparison presented in this manuscript on a given batch of colloids.

An additional transport experiment was conducted in a specially designed micromodel to microscopically examine the retention behavior of colloids in the sand. Details on the experimental micromodel procedures are given in Bradford et al. (*33*) and in the Supporting Information.

Results and Discussion

Table 2 presents values for the zeta potential of the sand and colloids under the various experimental conditions considered in this work. DLVO calculations were conducted using this information, and the predicted height of the energy barrier (Φ_{max}) to deposition in the primary minimum and the depth of the secondary minima (Φ_{2min}) are also presented in Table 2. The value of Φ_{max} is >1154 $k_B T_K$ (where k_B is the Boltzmann constant and T_K is the absolute temperature) in all cases, indicating unfavorable conditions for attachment in the primary minimum. The magnitude of Φ_{2min} increases with increasing IS due to compression of the diffuse double layer thickness.

Results from batch experiments using sand and colloids at $C_i = 3.6 \times 10^9$ N_c mL^{-1} and IS = 6, 31, 56, and 106 mM are given in Table 2. The background interference from the sand was very minor (<2% of C_i), and R_B of replicate

Downloaded by U OF CALIFORNIA RIVERSIDE on September 11, 2009 | http://pubs.acs.org
Publication Date (Web): August 11, 2009 | doi: 10.1021/es900840d

TABLE 2. Total Interaction Energy Parameters for 1.1 μm CML Colloids as a Function of IS[a]

IS (mM)	ζ_c (mV)	ζ_s (mV)	Φ_{max} (k_BT_K)	Φ_{2min} (k_BT_K)	R_B(%)
6	−107	−80	5824	−0.2	5
31	−91	−54	2709	−1.3	7
56	−96	−53	2608	−2.3	18
106	−44	−52	1154	−5.0	27

[a] The energy barrier height (Φ_{max}) and the depth of the secondary energy minima (Φ_{2min}) were obtained from DLVO calculations using zeta potentials for colloids (ζ_c) that were measured and for sand grains (ζ_s) that were estimated from the literature (*25, 26*). The average batch colloid retention (R_B) is also present at an initial colloid concentration of 3.6×10^9 N_c mL^{-1} for the various IS.

experiments varied <7% of C_i. The average value of R_B was low (5%) in the 6 mM system that was associated with a very shallow Φ_{2min} (-0.2 k_BT_K), suggesting that minimal colloid attachment occurred in the primary minimum as a result of chemical heterogeneity. Conversely, the average value of R_B increased with IS due to a greater magnitude of the Φ_{2min} (<27%). This suggests the potential for limited association of colloids in the Φ_{2min} (note that Φ_{max} was very high). Similar trends were observed from running replicate batch experiments at the lower C_i of 3.6×10^6 N_c mL^{-1}, with average values of R_B ranging from 9% to 29%. Hence, batch results were consistent with the DLVO calculations shown in Table 2 and demonstrate the existence of unfavorable attachment conditions.

Panels a−d of Figure 1 present representative colloid BTCs when q was approximately 0.1 cm min^{-1} and IS was 6, 31, 56, and 106 mM, respectively. Here, relative effluent concentrations (C/C_i) are plotted as a function of PV. Colloid retention increases with IS for a given value of C_i. This trend is expected (*15*), and is related to the increase in the depth of Φ_{2min} (Table 2). To study the influence of C_i on transport and retention, we conducted these experiments using C_i over a wide range (3.6×10^6 and 3.6×10^9 N_c mL^{-1}). It was observed that varying C_i over 3 orders of magnitude did not have much of an effect on the BTCs when the IS was 6 (Figure 1a) or 106 mM (Figure 1d). In contrast, the BTCs were dependent on C_i when the IS was 56 mM and especially sensitive when the IS was 31 mM. Additional transport experiments were therefore conducted using intermediate values of C_i equal to 3.6×10^7 and 3.6×10^8 N_c mL^{-1} when the IS was 31 and 56 mM, respectively. Under these conditions, lower values of C/C_i were observed with decreasing C_i. When the IS was 31 mM, the value of M_{BTC} varied from 5% at $C_i = 3.6 \times 10^6$ N_c mL^{-1} to 92% at $C_i = 3.6 \times 10^9$ N_c mL^{-1} (Table 1). Similar trends were observed in replicate experiments summarized in Table S1 of the Supporting Information. These observations demonstrate a coupled effect of IS and C_i on colloid retention, which may be explained as follows. The magnitude of Φ_{2min} and the fraction of colloids that interact with the solid phase increase with IS (Table 2). Little colloid interaction with the solid phase occurred when the IS was 6 mM, and no influence of C_i on retention was therefore observed. When colloids are weakly associated with the solid phase in a shallow Φ_{2min} (IS = 31 mM and 56 mM), we hypothesize that they are susceptible to removal via colloid collisions (especially when IS = 31 mM), which increase in frequency with C_i and therefore produce less retention. In contrast, when IS was 106 mM, no effect of C_i was observed because the depth of the Φ_{2min} is greater and it is more difficult for collisions to remove colloids from the solid.

Additional column experiments were conducted to better understand the effect of C_i on colloid transport and retention. The influence of hydrodynamics was investigated by running

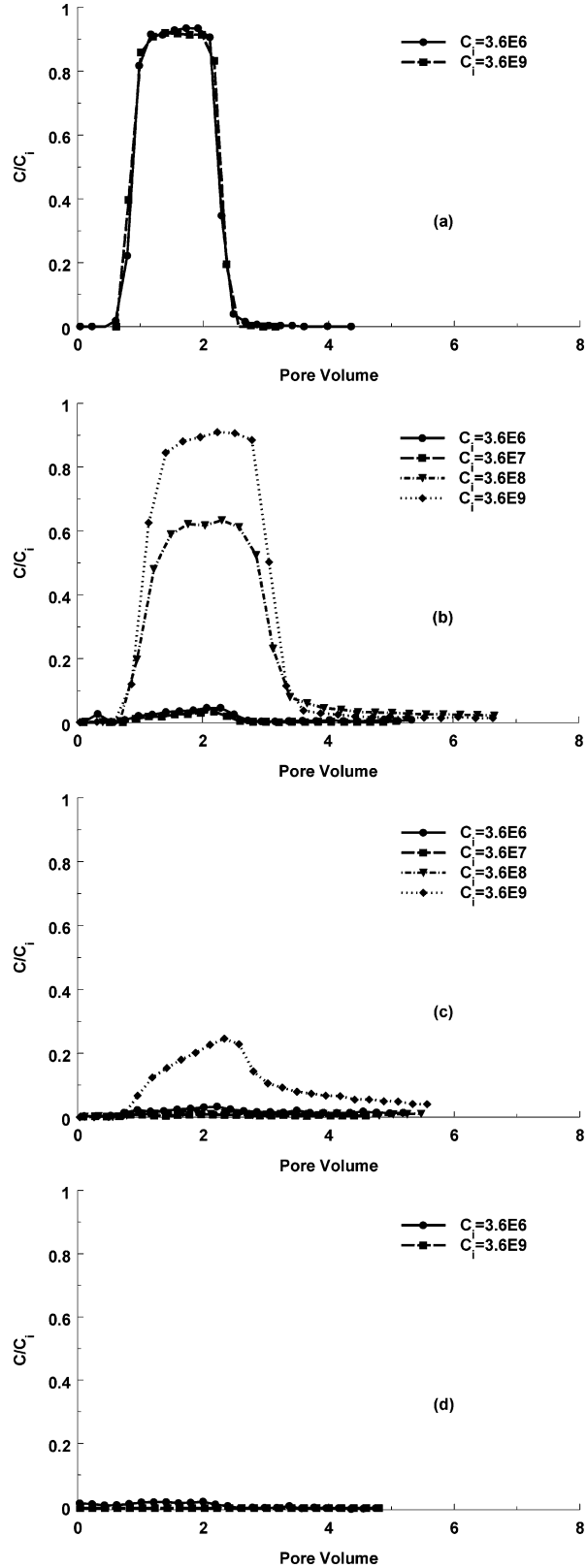

FIGURE 1. Breakthrough curves for 1.1 μm CML colloids in 150 μm Ottawa sand when $q \approx 0.1$ cm min^{-1}, pH 10, and IS = 6 (a), 31 (b), 56 (c), and 106 (d) mM. A wide range of C_i values were considered in these experiments, and specific values are indicated in the legend.

similar experiments to those shown in Figure 1 but at a velocity 5 times higher. Panels a and b of Figure 2 present representative colloid BTCs when q was approximately 0.5 cm min^{-1} and IS was 31 and 56 mM, respectively. The value

Downloaded by U OF CALIFORNIA RIVERSIDE on September 11, 2009 | http://pubs.acs.org
Publication Date (Web): August 11, 2009 | doi: 10.1021/es900840d

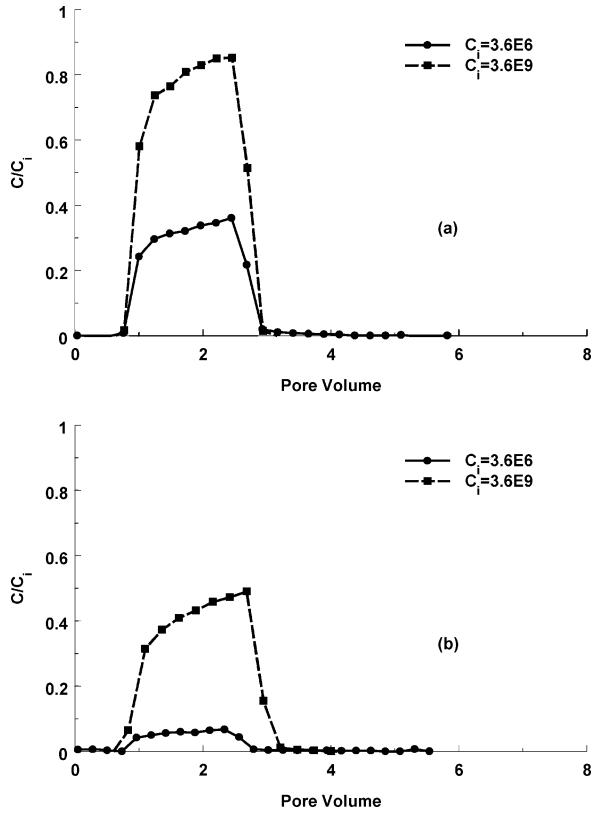

FIGURE 2. Breakthrough curves for 1.1 μm CML colloids in 150 μm Ottawa sand when $q \approx$ 0.5 cm min^{-1}, pH 10, and IS = 31 (a) and 56 (b) mM. A wide range of C_i values were considered in these experiments, and specific values are indicated in the legend.

of C_i was varied over 3 orders of magnitude (3.6×10^6 and 3.6×10^9 N_c mL^{-1}), and the BTCs showed a similar sensitivity to C_i as shown in panels b and c of Figure 1, with decreasing C_i resulting in lower peak values of C/C_i. Comparison of panels b and c of Figure 1 and panels a and b of Figure 2 at similar IS and C_i conditions and the corresponding value of M_{BTC} (Table 1 and Table S1 of the Supporting Information) indicates that the effect of C_i on colloid retention is also a function of the system hydrodynamics. Several plausible explanations for the coupled effect of q and C_i include the following. The kinetic energy of colloid collisions increases with the square of the particle trajectory velocity. Velocity will also influence the forces and torques that act on colloids near solid surfaces, with higher velocities leading to a smaller fraction of the solid surface that contributes to retention (*21*). Hence, an increase in velocity is expected to decrease colloid retention at a given C_i. This indeed occurs for systems with the greatest amount of relative retention; i.e., for the IS = 56 mM system at both C_i values and for IS = 31 mM system at $C_i = 3.6 \times 10^6$ N_c mL^{-1} (Table 1 and Table S1 of the Supporting Information). Consequently, the difference in the M_{BTC} at $C_i = 3.6 \times 10^6$ and 3.6×10^9 N_c mL^{-1} for the IS = 56 mM system is greater when q is highest (Figures 1c and 2b, Table 1, and Table S1 of the Supporting Information). In contrast, decreasing retention at a higher q in the $C_i = 3.6 \times 10^6$ N_c mL^{-1} and IS = 31 mM system reduces the difference in the M_{BTC} at the two C_i extremes because of relatively minor amounts of retention at the highest C_i.

A micromodel experiment was conducted to better identify locations of colloid retention and mechanisms of mass transfer under conditions when C_i had a large influence on colloid retention. These experiments mimicked conditions used in Figure 1b (IS = 31 mM) with $C_i = 3.6 \times 10^9$ N_c mL^{-1}. Figure 3 presents illustrative images of retained colloids in

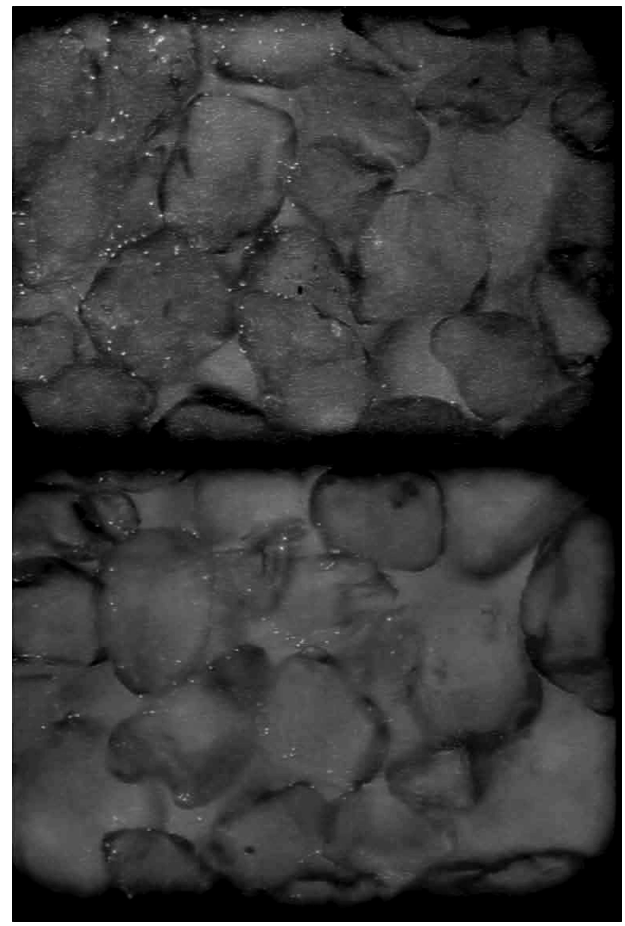

FIGURE 3. Illustrative microscopic images of retained 1.1 μm CML colloids in 150 μm Ottawa sand after recovery of the breakthrough curve; $q \approx$ 0.1 cm min^{-1}, pH 10, IS = 31 mM.

sand after recovery of the BTC. It was observed that colloid retention occurred primarily near grain−grain contact points that are associated with low velocities (*15*). Torque balance calculations presented by Torkzaban et al. (*15*) indicate that such locations are hydrodynamically favorable for colloid retention. Visual observations confirmed that mass transfer to these locations occurred by low advective and dispersive fluxes in the aqueous phase as well as along the solid phase. Only limited colloid retention was observed away from grain−grain contacts. Figure S2a of the Supporting Information and the associated discussion further substantiate these findings. Published fluorescent microscopy and X-ray microtomography studies have also demonstrated that colloids accumulate in narrow regions of pore spaces near the contacts of irregularly shaped sand grains (*23, 24, 33*−*37*) and may be translated on the solid surface in the presence of fluid drag (*38*) and a weak Φ_{2min}.

Additional experiments were conducted to study the influence of temporal changes in C_i on colloid retention. Figure 4 presents multipulse colloid BTCs with different step inputs of C_i indicated in the legend. These experiments were conducted when q was 0.5 cm min^{-1} and IS was 31 mM. When the input pulse of C_i was increased from 3.6×10^7 to 3.6×10^9 N_c mL^{-1}, a similar concentration effect was observed in C/C_i as was found in Figure 1b (increasing C_i resulted in a higher value of C/C_i). Conversely, when the input pulse of C_i was subsequently decreased from 3.6×10^9 to 3.6×10^8 to 3.6×10^7 N_c mL^{-1}, the concentration effect was largely eliminated, and values of C/C_i slowly approached a value of 0.95. In this case, the BTCs were slightly affected by background concentrations from higher C_i pulses, and this influenced the concentration tailing

Downloaded by U OF CALIFORNIA RIVERSIDE on September 11, 2009 | http://pubs.acs.org
Publication Date (Web): August 11, 2009 | doi: 10.1021/es900840d

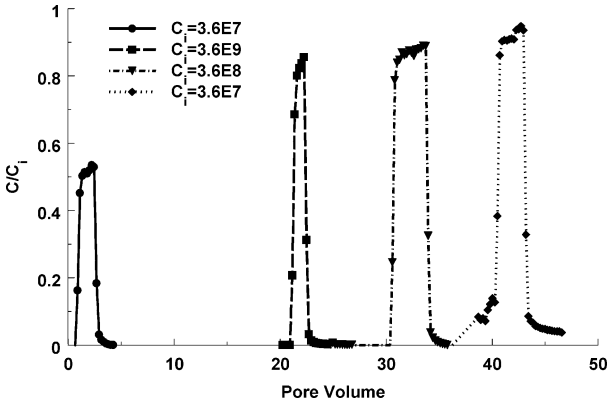

FIGURE 4. Multiple pulse breakthrough curves with different step inputs of C_i indicated in the legend. These experiments were conducted using 1.1 μm CML colloids in 150 μm Ottawa sand; $q \approx 0.5$ cm min^{-1}, pH 10, and IS = 31 mM.

behavior (<14% of C/C_i). Figure S3 of the Supporting Information provides additional transport data that show similar trends during transients in C_i at a different velocity. These observations indicate that as hydrodynamically favorable retention locations such as near grain−grain contacts become filled the concentration effect tended to disappear. This is analogous to chemically favorable sites being saturated. It implies a maximum cover of colloid retention under given system conditions (pore space geometry, hydrodynamics, and chemistry), which is independent of C_i. It should be noted that higher C_i will fill retention sites more rapidly than lower C_i.

To better understand the influence of C_i on the filling of retention sites, we need to examine the RPs. Figure 5 presents the RPs when q was approximately 0.1 cm min^{-1}, IS was 31 mM, and C_i was 3.6×10^6, 3.6×10^7, 3.6×10^8, and 3.6×10^9 N_c mL^{-1}. The corresponding BTCs for these systems were presented earlier in Figure 1b. Good mass balance was achieved in these experiments (90−103%). This suggests minimal errors were associated with our experimental protocols, and limited amounts of colloid attachment occurred in the primary minimum. In Figure 5a, relative concentrations ($N_c\ N_{ic}^{-1}$ g^{-1}, where N_{ic} is the number of colloids in a unit volume of C_i) of retained colloids are plotted as a function of depth from the column inlet. In Figure 5b, the absolute concentration of retained colloids (N_c g^{-1}) is plotted on a semilog scale as a function of depth to easily tell if the data is consistent with a first-order deposition model (log−linear). The shape of the RP in Figure 5 was highly dependent on C_i. Lower values of C_i produced nonexponential profiles (Figure 5b) and greater relative amounts of retention near the column inlet (Figure 5a). Conversely, higher values of C_i produced nearly exponential RP and higher amounts of absolute retention (Figure 5b and Figure S2b of the Supporting Information). These observations suggest a fixed number of retention locations, that the rate of filling of these sites was a function of C_i, and that the RPs were nonexponential with depth until the retention locations filled. Note, however, that colloid heterogeneity cannot explain the nonexponential RPs in Figure 5 because the only difference in the colloidal suspensions was due to concentration. Alternatively, one plausible explanation for this behavior is enhanced rates of colloid retention in low velocity regions (*39*) as was confirmed by micromodel observations. Additional discussion pertaining to the rather unusual shape of the RP for the $C_i = 3.6 \times 10^8$ N_c mL^{-1} system in Figure 5 is provided in Figure S2b and the text of the Supporting Information.

The fraction of the sand surface area (S_f) that contributed to colloid retention may be determined from the maximum

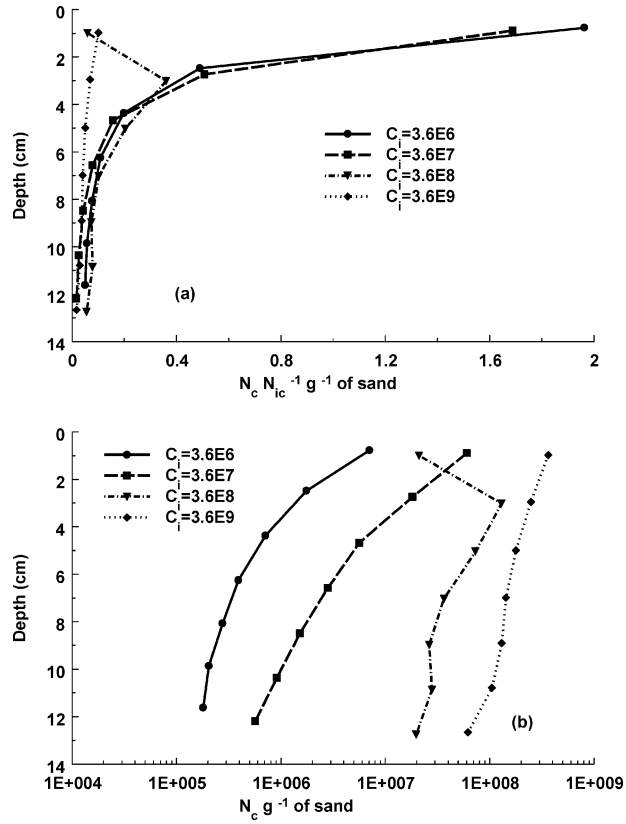

FIGURE 5. Final colloid retention profiles for 1.1 μm CML colloids in 150 μm Ottawa sand; $q \approx 0.1$ cm min^{-1}, pH 10, IS = 31 mM, and $C_i = 3.6 \times 10^6$, 3.6×10^7, 3.6×10^8, and 3.6×10^9 N_c mL^{-1}. (a) Relative soil concentrations ($N_c\ N_{ic}^{-1}$ g^{-1}) of colloids are plotted as a function of depth from the column inlet. (b) Soil concentration of colloids (N_c g^{-1}) is plotted on a semilog scale as a function of depth.

value of soil colloid concentration (S^{max}, $N_c\ M^{-1}$; M is mass), the geometrically estimated solid surface area of the sand (A_s, $L^2\ L^{-3}$; L is length), the cross-sectional area of the colloids (A_b, $L^2\ N_c^{-1}$), and the soil bulk density (ρ_b, $M\ L^{-3}$) as $S_f = (\rho_b A_b S^{max})/A_s$. The value of S^{max} in Figure 5b was approximately 3.6×10^8 N_c g^{-1}, and this yielded an estimate of $S_f = 2.3\%$. Hence, when IS = 31 mM, only a very small fraction of the solid surface area contributes to retention, and this observation further supports the contribution of pore structure on colloid retention under these conditions.

Bradford and Bettahar (*12*) observed similar effects of C_i on BTCs and RPs of 1.1 μm carboxyl colloids in various sized sands (360, 240, and 150 μm) when the system pH was approximately 7 and IS was 1 mM. This study applied approximately an equal mass of colloids to each column by adjusting the pulse duration for a particular value of C_i. For the same input mass of colloids, an increasing amount of colloid mass was recovered in the column effluent for higher values of C_i. To confirm this finding, we conducted additional colloid transport experiments when q was 0.25 cm min^{-1}, IS was 31 mM, and C_i was 3.6×10^7 and 3.6×10^8 N_c mL^{-1}. In this case, a similar input mass of colloids was injected into a column by adjusting the pulse duration. Figure S4 of the Supporting Information presents colloid BTCs from these experiments. Mass balance information indicates that 85% and 32% of the colloids were recovered in the effluent when C_i was 3.6×10^8 and 3.6×10^7 N_c mL^{-1}, respectively. Hence, the effect of C_i on colloid retention was not just a time- and concentration-dependent "filling" process.

The observed concentration effects on the BTCs and RPs shown in Figures 1, 2, 4, and 5, and Figures S3 and S4 of the

Downloaded by U OF CALIFORNIA RIVERSIDE on September 11, 2009 | http://pubs.acs.org
Publication Date (Web): August 11, 2009 | doi: 10.1021/es900840d

Supporting Information are hypothesized to be due to the following reasons: (i) time- and concentration-dependent filling of retention sites and (ii) concentration-dependent mass transfer of colloids to retention sites. Mass transfer to low velocity regions with enhanced retention was observed in the micromodel experiment to occur by advective and dispersive fluxes in the aqueous phase and rolling and sliding along on the solid surface. The collector efficiency (relative mass transfer of colloids to collector surfaces) is predicted to be independent of input concentration according to the filtration theory (*40*). Conversely, quantitative evaluation of mass transfer of colloids along the collector surface via rolling and/or sliding has not received much research attention. Higher input concentrations are expected to produce less relative mass transfer to retention locations due to increased numbers of collisions that knock weakly associated colloids off the solid phase. This hypothesis is supported by the observed dependence of BTCs on C_i (number of collisions) and adhesive and fluid drag forces (an optimal value for rolling mass transfer will depend on IS, pH, and q). Micromodel observations also support this conceptual picture.

Results from this study have important implications for predicting the fate of colloids and microorganisms and colloid-associated contaminants in subsurface environments that are unfavorable for attachment. Specifically, results indicate that only a small fraction of the porous media may contribute to colloid retention, and that once this fraction is filled, then enhanced transport of colloids is likely. Hence, conclusions about the fate of colloids that are derived from transport experiments conducted under clean bed initial conditions or without equilibration with natural background colloids are unlikely to accurately reflect their true long-term transport potential. Furthermore, clean bed transport experiments under unfavorable attachment conditions are expected to be very sensitive to the suspension concentration (including natural background levels), and caution is therefore warranted when comparing with results in other conditions.

Downloaded by U OF CALIFORNIA RIVERSIDE on September 11, 2009 | http://pubs.acs.org
Publication Date (Web): August 11, 2009 | doi: 10.1021/es900840d

Acknowledgments

We thank Alan Nguyen and Lorena Altamirano for their help in conducting the transport experiments. This research was supported by the United States Department of Agriculture (USDA), Agricultural Research Service (ARS), National Program (NP) 206 and the Cooperative State Research, Education, and Extension Service (CSREES), National Research Initiative (NRI), Grant 2006-02541.

Supporting Information Available

A brief description and discussion of (i) the protocol for the packed column and micromodel experiments, (ii) information on replicate column experiments (Table S1 and Figure S1), (iii) a colloid BTC and RP following a decrease in the IS from 31 to 6 mM and two flow interruptions during the elution phase (Figure S2), (iv) additional BTCs for transient C_i experiments (Figure S3), and (v) a comparison of colloid BTCs that apply similar input mass of colloids at different C_i values by adjusting the pulse duration (Figure S4). This material is available free of charge via the Internet at http://pubs.acs.org.

Literature Cited

(1) Kim, J. I. Actinide colloid generation in groundwater. *Radiochim. Acta* **1991**, *52/53*, 71–81.
(2) McCarthy, J. F.; Degueldre, C. Sampling and characterization of colloids and particles in groundwater for studying their role in contaminant transport. In *Environmental Particles*; Buffle, J., van Leeuwen, H. P., Eds.; Lewis Publishers: Boca Raton, FL, 1993; Vol. 2, pp 247−315.
(3) Ryan, J. N.; Elimelech, M. Colloid mobilization and transport in groundwater. *Colloids Surf., A* **1996**, *107*, 1–56.
(4) De Novio, N. M.; Saiers, J. E.; Ryan, J. N. Colloid movement in unsaturated porous media: Recent advances and future directions. *Vadose Zone J.* **2004**, *3*, 338–351.
(5) Tan, Y.; Gannon, J. T.; Baveye, P.; Alexander, M. Transport of bacteria in an aquifer sand: Experiments and model simulations. *Water Resour. Res.* **1994**, *30*, 3243–3252.
(6) Lindqvist, R.; Cho, J. S.; Enfield, C. G. A kinetic model for cell density dependent bacterial transport in porous media. *Water Resour. Res.* **1994**, *30*, 3291–3299.
(7) Liu, D.; Johnson, P. R.; Elimelech, M. Colloid deposition dynamics in flow-through porous media: Role of electrolyte concentration. *Environ. Sci. Technol.* **1995**, *29*, 2963–2973.
(8) Camesano, T. A.; Logan, B. E. Influence of fluid velocity and cell concentration on the transport of motile and nonmotile bacteria in porous media. *Environ. Sci. Technol.* **1998**, *32*, 1699–1708.
(9) Pandya, V. B.; Bhuniya, S.; Khilar, K. C. Existence of a critical particle concentration in plugging of a packed bed. *AIChE J.* **1998**, *44*, 978–981.
(10) Camesano, T. A.; Unice, K. M.; Logan, B. E. Blocking and ripening of colloids in porous media and their implications for bacterial transport. *Colloids Surf., A* **1999**, *160*, 291–308.
(11) Ramachandran, V.; Fogler, H. S. Plugging by hydrodynamic bridging during flow of stable colloidal particles within cylindrical pores. *J. Fluid Mech.* **1999**, *385*, 129–156.
(12) Bradford, S. A.; Bettahar, M. Concentration dependent colloid transport in saturated porous media. *J. Contam. Hydrol.* **2006**, *82*, 99–117.
(13) Johnson, P. R.; Elimelech, M. Dynamics of colloid deposition in porous media: Blocking based on random sequential adsorption. *Langmuir* **1995**, *11*, 801–812.
(14) Bradford, S. A.; Torkzaban, S. Colloid transport and retention in unsaturated porous media: A review of interface, collector, and pore scale processes and models. *Vadose Zone J.* **2008**, *7*, 667–681.
(15) Torkzaban, S.; Tazehkand, S. S.; Walker, S. L.; Bradford, S. A. Transport and fate of bacteria in porous media: Coupled effects of chemical conditions and pore space geometry. *Water Resour. Res.* **2008**, *44*, W04403, doi:10.1029/2007WR006541.
(16) Johnson, W. P.; Li, X.; Yal, G. Colloid retention in porous media: Mechanistic confirmation of wedging and retention in zones of flow stagnation. *Environ. Sci. Technol.* **2007**, *41*, 1279–1287.
(17) Herzig, J. P.; Leclerc, D. M.; LeGoff, P. Flow of suspension through porous media: Application to deep filtration. *Ind. Eng. Chem.* **1970**, *62*, 129–157.
(18) McDowell-Boyer, L. M.; Hunt, J. R.; Sitar, N. Particle transport through porous media. *Water Resour. Res.* **1986**, *22*, 1901–1921.
(19) Bradford, S. A.; Simunek, J.; Bettahar, M.; van Genuchten, M. Th.; Yates, S. R. Significance of straining in colloid deposition: Evidence and implications. *Water Resour. Res.* **2006**, *42*, W12S15, doi:10.1029/2005WR004791.
(20) Bradford, S. A.; Torkzaban, S.; Walker, S. L. Coupling of physical and chemical mechanisms of colloid straining in saturated porous media. *Water Res.* **2007**, *41*, 3012–3024.
(21) Torkzaban, S.; Bradford, S. A.; Walker, S. L. Resolving the coupled effects of hydrodynamics and DLVO forces on colloid attachment to porous media. *Langmuir* **2007**, *23*, 9652–9660.
(22) Shen, C.; Huang, Y.; Li, B.; Jin, Y. Effects of solution chemistry on straining of colloids in porous media under unfavorable conditions. *Water Resour. Res.* **2008**, *44*, W05419, doi:10.1029/2007WR006580.
(23) Bradford, S. A.; Simunek, J.; Walker, S. L. Transport and straining of *E. coli* O157:H7 in saturated porous media. *Water Resour. Res.* **2006**, *42*, W12S12, doi:10.1029/2005WR4805.
(24) Tong, M.; Ma, H.; Johnson, W. P. Funneling of flow into grain-to-grain contacts drives colloid−colloid aggregation in the presence of an energy barrier. *Environ. Sci. Technol.* **2008**, *42*, 2826–2832.
(25) Elimelech, M.; Nagai, M.; Ko, C.-H.; Ryan, J. N. Relative insignificance of mineral grain zeta potential to colloid transport in geochemically heterogeneous porous media. *Environ. Sci. Technol.* **2000**, *34*, 2143–2148.
(26) Redman, J. A.; Walker, S. L.; Elimelech, M. Bacterial adhesion and transport in porous media: Role of the secondary energy minimum. *Environ. Sci. Technol.* **2004**, *38*, 1777–1785.
(27) Derjaguin, B. V.; Landau, L. D. Theory of the stability of strongly charged lyophobic sols and of the adhesion of strongly charged particles in solutions of electrolytes. *Acta Physicochim. U.S.S.R.* **1941**, *14*, 733–762.
(28) Verwey, E. J. W.; Overbeek, J. Th. G. *Theory of the Stability of Lyophobic Colloids*. Elsevier: Amsterdam, 1948.

(29) Hogg, R.; Healy, T. W.; Fuerstenau, D. W. Mutual coagulation of colloidal dispersions. *Trans. Faraday Soc.* **1966**, *62*, 1638–1651.
(30) Gregory, J. Approximate expression for retarded van der Waals interaction. *J. Colloid Interface Sci.* **1981**, *83*, 138–145.
(31) Bergendahl, J.; Grasso, D. Prediction of colloid detachment in a model porous media: Thermodynamics. *AIChE J.* **1999**, *45*, 475–484.
(32) Bradford, S. A.; Yates, S. R.; Bettahar, M.; Šimùnek, J. Physical factors affecting the transport and fate of colloids in saturated porous media. *Water Resour. Res.* **2002**, *38*, 1327, doi:10.1029/2002WR001340.
(33) Bradford, S. A.; Šimùnek, J.; Bettahar, M.; Tadassa, Y. F.; van Genuchten, M. Th.; Yates, S. R. Straining of colloids at textural interfaces. *Water Resour. Res.* **2005**, *41*, W10404, doi:10.1029/2004WR003675.
(34) Xu, S.; Gao, B.; Saiers, J. E. Straining of colloidal particles in saturated porous media. *Water Resour. Res.* **2006**, *42*, W12S16, doi:10.1029/2006WR004948.
(35) Li, X.; Lin, C.-L.; Miller, J. D.; Johnson, W. P. Pore-scale observation of microsphere deposition at grain-to-grain contacts over assemblage-scale porous media domains using x-ray microtomography. *Environ. Sci. Technol.* **2006**, *40*, 3762–3768.
(36) Yoon, J. S.; Germaine, J. T.; Culligan, P. J. Visualization of particle behavior with a porous medium: Mechanisms for particle filtration and retardation during downward transport. *Water Resour. Res.* **2006**, *42*, W06417, doi:10.1029/2004WR003660.
(37) Gaillard, J. F.; Chen, C.; Stonedahl, S. H.; Lau, B. L. T.; Keane, D. T.; Packman, A. I. Imaging of colloidal deposits in granular porous media by X-ray difference micro-tomography. *Geophys. Res. Lett.* **2007**, *34*, L18404, doi:10.1029/2007GL030514.
(38) Kuznar, Z. A.; Elimelech, M. Direct microscopic observation of particle deposition in porous media: Role of the secondary energy minimum. *Colloids Surf., A* **2007**, *294*, 156–162.
(39) Bradford, S. A.; Torkzaban, S.; Leij, F.; Simunek, J.; van Genuchten, M. Th. Modeling the coupled effects of pore space geometry and velocity on colloid transport and retention. *Water Resour. Res.* **2009**, *45*, W02414. doi:10.1029/2008WR007096.
(40) Yao, K. M.; Habibian, M. T.; O'Melia, C. R. Water and waste water filtration: Concepts and applications. *Environ. Sci. Technol.* **1971**, *5*, 1105–1112.

ES900840D

Downloaded by U OF CALIFORNIA RIVERSIDE on September 11, 2009 | http://pubs.acs.org
Publication Date (Web): August 11, 2009 | doi: 10.1021/es900840d